*Thermochimica Acta*, 202 (1992) 269–280
Elsevier Science Publishers B.V., Amsterdam

# Acid properties of silica and alumina surfaces as probed by thermogravimetry and differential scanning calorimetry of temperature-programmed desorption of pyridine

H.M. Ismail, S.A.A. Mansour and M.I. Zaki

*Chemistry Department, Faculty of Science, Minia University, El-Minia (Egypt)*

(Received 19 August 1991)

## Abstract

Thermogravimetry and differential scanning calorimetry of the temperature-programmed desorption of pyridine from silica and alumina surfaces were carried out. Quantitative information on the concentration and strength of the surface acid sites was derived from the results obtained. The principal objective was to find out the merits and drawbacks of the two techniques in studying the acid–base properties of solid surfaces. The investigation shows that the use of these techniques can be successful provided that a number of requirements is fulfilled. These requirements were characterized and are discussed.

## INTRODUCTION

The acid–base properties of solid surfaces influence their catalytic [1,2] and catalyst supporting [3,4] functions. In order to understand the mechanism by which these functions are performed, it is necessary to have available quantitative information on the concentration and strength of the surface acid and basic sites. Therefore, a number of experimental methods have been devised [1,5,6], including titrimetric, spectroscopic and thermoanalytic techniques, to accomplish this objective. As a common feature, the application of any of these techniques necessitates the use of acid or base probe molecules.

Comparative studies [7] have led to the formulation of the following list of requirements to be met by a successful quantitative method: (i) the interaction between the probe molecule and the different types of acid or basic sites should be reliably identified and discerned; (ii) the strength of the individual sites should be determinable numerically, on a defined scale; and (iii) the concentration of each type of site should be independently determinable.

---

*Correspondence to:* M.I. Zaki, Chemistry Department, Faculty of Science, Minia University, El-Minia, Egypt.

It has been concluded [7] that the above requirements are largely met by spectroscopic techniques, in particular the infra-red (IR) spectroscopy of adsorbed species [8,9]. Thermoanalytical techniques were considered [7] incapable of differentiating between the interactions of the probe with the different acid and basic sites. Therefore, few thermoanalytical studies of the acid–base properties of surfaces have been reported [10,11]. However, thermogravimetry has been found [7] to be necessary to complement the IR data with regard to the surface concentration of the sites.

The aim of the present investigation was to demonstrate the merits and drawbacks of thermoanalytical techniques in studying the acid–base properties of solid surfaces. To accomplish this objective: (i) silica and alumina surfaces, which have been probed for acid–base properties by means of a wide range of analytical techniques [7,12], were adopted as study cases; (ii) pyridine was used as the probe molecule; (iii) non-isothermal thermogravimetric (TG) and differential scanning calorimetric (DSC) measurements were made on the test materials, both before and after pyridine adsorption; (iv) isothermal gravimetry was undertaken to follow the adsorption/desorption of pyridine at various temperatures in dynamic vacuum; and (v) the results were correlated with published data obtained using other techniques.

## EXPERIMENTAL

### *Materials*

The silica (213 $m^2\ g^{-1}$ Si) and $\gamma$-alumina (110 $m^2\ g^{-1}$ Al) used were Degussa Aerosil-200 and Aluminiumoxide C, respectively. Prior to application, these materials were heated at 450°C for 2 h, in a stream (30 $cm^3\ min^{-1}$) of dry $N_2$ (Egyptian Company of Industrial Gases, Helwan/Cairo; nominal purity 99.8%) previously dried by passing through cold traps (−195°C) packed with molecular sieve (4A) and self-indicating silica gel (Merck). Subsequently, the temperature was levelled off, and the samples withdrawn from the furnace (while at 200°C) and kept dry over $CaCl_2$.

The pyridine adsorbate was an AR grade product of Koch-light laboratories Ltd. (Buckinghamshire, UK).

### *Pyridine adsorption*

Portions of silica and alumina were transferred, in air, from the drying desiccator into another desiccator containing liquid pyridine. The transfer was done quickly in order to minimize the contact time with the ambient atmosphere. The materials were maintained in contact with the pyridine vapour, at room temperature, for 4 weeks, prior to analysis. For simplicity, the pyridine covered samples are denoted here by Py/Si and Py/Al.

### *Isothermal gravimetry*

The temperature dependence of pyridine adsorption/desorption on the test materials (silica and alumina) was determined gravimetrically, using an air-thermostatted (35 ± 0.5°C), all-glass vacuum line equipped with micromanometers and high sensitivity (38 cm $g^{-1}$) silica springs (Springham, UK). Variations in the spring elongation, as a result of the adsorbent weight changes, were measured by means of a cathetometer (The Precision Tool and Instrument Co., UK) capable of giving readings accurate to within ±0.01 cm.

Portions (250–300 mg) of the dried test materials were outgassed in situ at $10^{-5}$ Torr and 200°C for 2 h, and then cooled to 35°C under dynamic vacuum. Subsequently, the samples were exposed to 6 Torr of pyridine vapour, which was withdrawn in situ from Py deaerated by freeze–pump–thaw cycles. Following a 2-h exposure, the gas phase was pumped off until a constant weight (i.e. constant spring elongation) was obtained. The temperature was then elevated in vacuo to a certain value in the range 100–300°C, and maintained until a constant weight was reached (1–3 h). Thereafter, the temperature was levelled off to 35°C, and the spring elongation, and hence the amount of irreversibly held pyridine (in milligrams per gram), was determined.

The heating was facilitated (at 30°C $min^{-1}$) by a home-made temperature-controlled cylindrical furnace, and the temperature was measured using a Cole-Parmer Digi-Sense thermometer equipped with a type-K thermocouple. The thermocouple tip was placed at the nearest possible point to the test sample.

### *Non-isothermal gravimetry*

Uncoated and pyridine coated test samples were subjected to TG analysis over the temperature range from ambient to 400°C (at 30°C $min^{-1}$) in a stream of dry $N_2$ (30 $cm^3$ $min^{-1}$). The TG curves were automatically recorded on a Model 30H Shimadzu unit (Japan). A thermal differentiation (TD) function was activated simultaneously to the TG measurements in order to improve the resolution.

### *Differential scanning calorimetry*

DSC curves were obtained (temperature range ambient to 400°C, heating rate 30°C $min^{-1}$) for uncoated and pyridine coated test samples, in a stream of dry $N_2$ (30 $cm^3$ $min^{-1}$), using the above indicated Shimadzu unit. The heat of fusion (28.5 J $g^{-1}$) [13] of Specpure indium (at 156.5°C) was adopted for the curve calibration.

### *Quantitative calculations*

The surface OH content of the dried test samples was calculated (in milligram per gram) from the TG-determined total weight loss at 400°C, after subtracting the weight loss due to physically adsorbed water (TG determined near 100°C) (for details see ref. 14). The OH population (number of OH groups per square nanometre of sample surface, OH $\mathrm{nm}^{-2}$) was then derived on basis of the specific surface area (square metres per gram).

Similarly, the population of adsorbed pyridine molecules (number of pyridine molecules per square nanometre of sample surface, Py $\mathrm{nm}^{-2}$) was calculated; however, using the equation

$$\mathrm{Py\ nm}^{-2} = (L - l) \times 6.02 \times 10^{23}/(W_0 - L) \times 79 \times S_a \times 10^{18} \qquad (1)$$

where $L$ and $l$ are the TG-determined weight losses (milligram) for the pyridine coated and uncoated test samples, respectively, at a given temperature (see Fig. 1, for example), $W_0$ is the initial sample weight (milligram), 79 is the molecular weight of pyridine, and $S_a$ is the surface area of the sample (square metres per gram).

The enthalpy change ($\Delta H$ in kilojoule per mole) occurring on desorption of pyridine over a given temperature range ($T$) was derived from the DSC curves of the uncoated and pyridine coated test samples as

$$\Delta H = (A - a) \times K/(L - l) \qquad (2)$$

where $A$ and $a$ are the DSC peak areas (square centimetres) for the pyridine coated and uncoated test samples, respectively, at $T$ (see Fig. 1, for example), $L$ and $l$ are the TG-determined weight losses (milligram) at $T$, as defined above, $K$ is the calibration constant (joules per square centimetre), which was calculated from the DSC peak area ($A_s$) corresponding to the heat of fusion ($\Delta H_s$) of $m_s$ grams of indium, according to the equation

$$K = (m_s/A_s) \times \Delta H_s$$

It is worth mentioning that the peak areas were determined using a planimeter, following a deconvolution of the composite peaks in the DSC curves (see Figs. 1 and 2).

## RESULTS AND DISCUSSION

### *Literature background*

Metal oxide surfaces expose Lewis (L) and Brønsted (B) acid sites. The former sites are associated with coordinatively unsaturated metal ions, whereas the latter sites are proton donor OH groups [7]. Moreover, OH

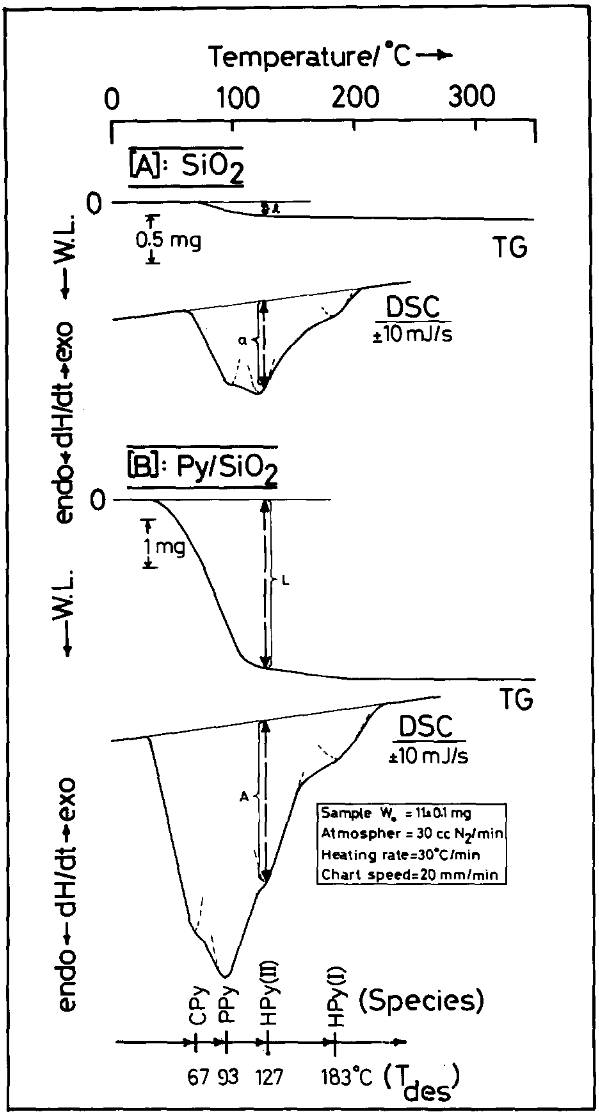

Fig. 1. TG and DSC curves recorded for silica (A) and pyridine/silica (B). The bottom line scales the pyridine adsorbed species to their desorption temperature regimes as defined by means of a thermal differentiator (this also applies to Fig. 2). The vertical dashed lines specify quantities used in the sample calculation described in the experimental section.

groups incapable of donating protons, but accumulating a net positive charge, may act as hydrogen bond donors [15]. These are provisionally considered as weak B sites [1,7]. The strength of L sites is controlled by the extent of coordination unsaturation and symmetry of the metal ion, which are intimately related to the number and spatial distribution of its nearest neighbours [12]. The strength of B sites, however, is governed by the mode of bonding of the OH group to the surface as well as by the coordination

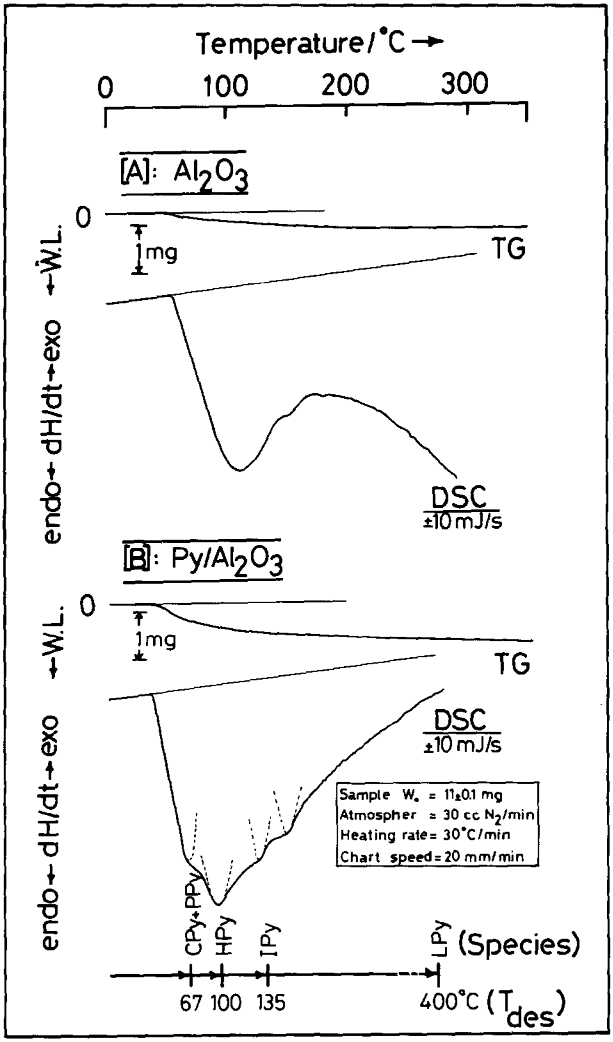

Fig. 2. TG and DSC curves recorded for alumina (A) and pyridine/alumina (B).

symmetry of the coordinating metal site [16]. Therefore, it is possible that different strength L and B sites are generated on a given surface.

Silica surfaces only expose weak B sites, which are hydrogen bond donor silanol groups (i.e. terminal Si–OH groups) [17]. In contrast, alumina surfaces also expose L sites associated with coordinatively unsaturated $Al^{3+}$ sites [18]. Having been pre-exposed to water vapour, alumina surfaces may also exhibit proton-donor B sites originating from coordinated water molecules ($Al^{3+} \longleftarrow O{<}^{H}_{H^{\delta+}}$ [1]). Well-accepted models of $\gamma$-$Al_2O_3$ surfaces [16,19] agree on the existence of five different types of OH groups and at least two different L sites (tetrahedrally and octahedrally coordinated $Al^{3+}$ ions). A low-temperature IR spectroscopic study of adsorbed

CO indicated that only a minor proportion of the surface OH groups of alumina (bridge bonded) are capable of hydrogen bonding, whilst the majority of the OH groups (mostly terminally bound) are rather basic in character [20]. Recent IR studies have disclosed that only one type of L site is detectable, following a mild dehydroxylation at moderate temperatures ($\leqslant$ 500°C, in vacuo) [21]. It is not until an intensive dehydroxylation is effected near 700°C that the second type of L site becomes detectable [18]. Very recently, however, the dehydroxylation of $\gamma$-$Al_2O_3$ at extremely high temperatures ($\geqslant$ 900°C) has been found to generate a third type of L site [22], i.e. a metal ion in the neighbourhood of an oxygen vacancy.

Pyridine has a large dipole moment ($\mu = 2.2$ D) [7]. Therefore, it is a "hard" base molecule and hence cannot discriminate between weak and strong acid sites [7]. In the IR method, the analytical frequency shifts $\Delta\nu$(CCN) of coordinated pyridine (LPy) are similar, irrespective of the nature of the L site [7]. Pyridine is capable of accepting protons, thus giving rise to pyridinium ion-paired (IPy) with the proton-donor sites [1,7,12]. Pyridine can also accept hydrogen bonds to form HPy species with weak B sites. Pyridine is chemically stable on silica surfaces even at temperatures as high as 400°C [12]. However, on alumina surfaces, and at $>$ 300°C, pyridine is chemically modified into $\alpha$-pyridone due to nucleophilic attack by basic Al–OH groups [23].

### *Thermogravimetry and population of acid sites*

Thermogravimetry of silica and alumina (i.e. uncoated) samples was carried out non-isothermally, and the curves obtained are shown in Figs. 1 and 2, respectively. The surface OH populations derived from these curves are approximately 1 and 11 OH $nm^{-2}$ for silica and alumina, respectively. The value determined for silica is much less than that (5–6 OH $nm^{-2}$) [17] reported for completely hydroxylated silicas. However, the population determined for alumina is very close to that (10–11 OH $nm^{-2}$) [16,24] reported for completely hydroxylated $\gamma$-$Al_2O_3$. It is worth recalling, in this respect, that both the silica and the alumina samples were similarly preheated at 450°C and briefly brought into contact with the ambient air atmosphere while being transferred to the analysis unit. Thus the fact that alumina is much more readily rehydrated than is silica [25] at room temperature may be of importance here. This factor is also reflected by the higher weight loss due to water physically adsorbed (near 100°C) on alumina (Fig. 2) than on silica (Fig. 1), although the latter material has a higher surface area (213 $m^2$ $g^{-1}$) than the former (110 $m^2$ $g^{-1}$).

Thermogravimetry of Py/Si and Py/Al (i.e. pyridine coated samples) was carried out both non-isothermally and isothermally. The non-isothermal measurements resulted in the TG curves shown in Figs. 1 and 2 for Py/Si and Py/Al, respectively. The quantitative data derived from these

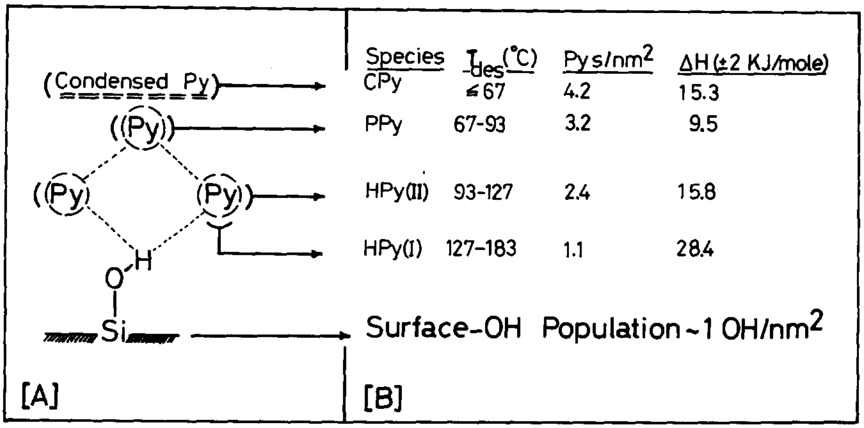

| Species | $T_{des}$(°C) | Pys/nm$^2$ | ΔH (±2 KJ/mole) |
|---|---|---|---|
| CPy | ≤67 | 4.2 | 15.3 |
| PPy | 67-93 | 3.2 | 9.5 |
| HPy(II) | 93-127 | 2.4 | 15.8 |
| HPy(I) | 127-183 | 1.1 | 28.4 |

Surface-OH Population ~1 OH/nm$^2$

Fig. 3. (A) A model structure for the pyridine layer adsorbed on silica. (B) Population (Py nm$^{-2}$), desorption temperature range ($T_{des}$) and enthalpy ($\Delta H$) for the various pyridine species: CPy, condensed; PPy, physisorbed; HPy (II and I), hydrogen bonded.

curves are summarized in Figs. 3(B) and 4(B), respectively. The data derived from the isothermal measurements are compiled for both systems in Table 1. Before looking at the results, it must be emphasized that there are significant experimental differences between the two modes of measurement. In the isothermal mode, the test samples were pretreated and exposed to the pyridine vapour in situ. Moreover, the isothermal measurements facilitate obtaining equilibrium quantities; such conditions are not accomplished when dealing with the non-isothermal measurements.

The data shown for Py/Si in Fig. 3(B), which were derived from the TG curves exhibited in Fig. 1, indicate the existence of various pyridine adsorbed species. The differences in magnitude between the temperature

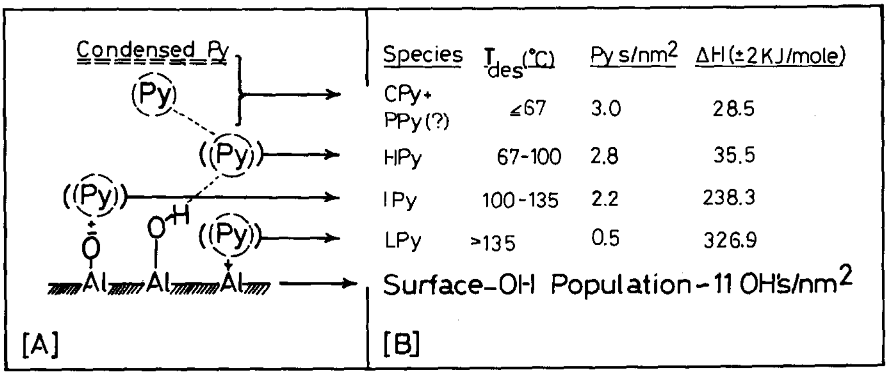

| Species | $T_{des}$(°C) | Pys/nm$^2$ | ΔH (±2 KJ/mole) |
|---|---|---|---|
| CPy+<br>PPy(?) | ≤67 | 3.0 | 28.5 |
| HPy | 67-100 | 2.8 | 35.5 |
| IPy | 100-135 | 2.2 | 238.3 |
| LPy | >135 | 0.5 | 326.9 |

Surface-OH Population ~11 OH's/nm$^2$

Fig. 4. (A) A model structure for the pyridine layer adsorbed on alumina. (B) Population (Py nm$^{-2}$), desorption temperature range ($T_{des}$) and enthalpy ($\Delta H$) for the various pyridine species: CPy, PPy, HPy and IPy, ion-paired; LPy, coordinated.

TABLE 1

Specific (mg $g^{-1}$) and intrinsic (Py $nm^{-2}$) adsorption data of pyridine on silica and alumina test samples [a] as determined gravimetrically (at 35°C), following heating at various temperatures in vacuo until constant weight was reached

| Temperature (°C) | Silica | | Alumina | |
|---|---|---|---|---|
| | Specific [b] (mg $g^{-1}$) | Intrinsic [c] (Py $nm^{-2}$) | Specific [b] (mg $g^{-1}$) | Intrinsic [c] (Py $nm^{-2}$) |
| 35 | 82 | 2.9 | 169 | 11.7 |
| 100 | 30 | 1.1 | 24 | 1.7 |
| 150 | 0 | 0 | 16 | 1.1 |
| 200 | – | – | 11 | 0.8 |
| 250 | – | – | 11 | 0.8 |

[a] Test samples were pretreated in situ at 200°C and $10^{-5}$ Torr until constant weight was reached.

[b] Rounded to the nearest integer.

[c] Number of pyridine molecules per square nanometre of the silica (213 $m^2$ $g^{-1}$) and alumina (110 $m^2$ $g^{-1}$) surface.

ranges indicated for the desorption of the different species suggest that they form various desorption states [12]. It is suggested that these are (Fig. 3): condensed pyridine (CPy), at $\leqslant$ 67°C; physisorbed pyridine (PPy), at 67–93°C; and hydrogen bonded pyridine (HPy), at 93–127°C (II) and at 127–183°C (I). The formation of such species reveals [17] that silica surfaces only expose weak B sites. The relative proportions of the calculated population for each pyridine species may give rise to the structure modelled for the adsorbed layer in Fig. 3(A). Two types of HPy species are suggested: (II) two pyridine molecules bound to a single OH group; and (I) one pyridine molecule bound to a single OH group. This is compatible with the paucity of hydroxyl groups on the test sample. It is noteworthy that the ratio of the population of HPy (I) to that of surface hydroxyl groups is very close to unity (Fig. 3(B)).

The above-described picture is further supported by the data derived from the isothermal gravimetry of Py/Si (Table 1). The population of irreversibly held pyridine molecules at 35°C, namely 2.9 Py $nm^{-2}$, is close to that (3.2 Py $nm^{-2}$) found to desorb non-isothermally at 67–93°C. As the CPy and PPy species cannot withstand evacuation at 35°C [26], the irreversibly held molecules are most probably of the suggested HPy species (Fig. 3), which desorb completely at temperatures of $\geqslant$ 150°C (Table 1). Similar behaviour is found at 183°C in the non-isothermal gravimetry of Py/Si (Fig. 1). The isothermal measurements further confirm that the relatively most stable hydrogen bonded pyridine molecules are those forming the HPy(I) species (i.e. Py : OH $\approx$ 1).

The data summarized in Fig. 4(B) for Py/Al were derived from the TG curves exhibited in Fig. 2. They account for the desorption of various pyridine species: CPy and/or PPy at $\leqslant 67$°C; HPy at 67–100°C; IPy at 100–135°C; and LPy at $> 135$°C. Figure 4(B) also shows the population of each type of pyridine species and the structure of the adsorbed layer is modelled in Fig. 4(A). The data derived from the isothermal gravimetry of Py/Al are given in Table 1.

The above results lead to the following observations with regard to the nature of acid sites on alumina. As expected [16,19], the results account for the exposure of weak (HPy) and strong (IPy) B sites, as well as L sites (LPy). The isothermally determined population of irreversibly held pyridine at 35°C (11.7 Py $\mathrm{nm}^{-2}$) is significantly higher than the non-isothermally determined values (Fig. 4(B)). Bearing in mind the experimental differences between the two approaches (see above), this observation may point to the influence of the water coverage on the test sample prior to isothermal gravimetry.

The water molecules would be coordinated to L sites and hydrogen bonded to B sites, thus making a considerable proportion of them inaccessible to the pyridine molecules [1,12]. Coordinated water molecules generate the strong B sites responsible for the formation of the IPy species [1,12]. In agreement with this, the population (2.2 Py $\mathrm{nm}^{-2}$) of the desorbing pyridine species at 100–135°C, as determined non-isothermally, is higher than that (1.1 Py $\mathrm{nm}^{-2}$) determined isothermally for irreversibly held pyridine at 150°C. Thus the latter amount may relate exclusively to the LPy species, which is shown (both isothermally and non-isothermally) to persist against desorption up to higher temperatures (Fig. 4(B) and Table 1). IR studies of pyridine adsorption on alumina surfaces (e.g. ref. 27) have shown the stability of LPy species on heating (in vacuo) up to 500°C. Other studies [23], however, have indicated that the LPy species on alumina suffers a chemical modification to $\alpha$-pyridone at 300°C. In any case, the markedly low population of LPy species (0.8 Py $\mathrm{nm}^{-2}$) as isothermally determined at 200–250°C (Table 1), which should accordingly [23] be due to unmodified pyridine, indicates clearly that the pretreatment of the test sample does not suffice to generate many L sites on the surface. This observation is in line with the results of earlier studies [21,22].

## *Differential scanning calorimetry and strength of acid sites*

The DSC curves obtained for pyridine coated and uncoated silica and alumina are shown in Figs. 1 and 2, respectively. The enthalpy changes ($\Delta H$ in kilojoules per mole) calculated therefrom for the desorption of the various pyridine species formed on silica and alumina are summarized in Figs. 3(B) and 4(B), respectively. The values are considered to show the relative strengths of the acid sites involved.

Generally speaking, the differences between the $\Delta H$ values calculated can be considered to be indicative of different desorption states [12]. In the case of Py/Si, the range of $\Delta H$ values (Fig. 3(B)) lies well within the distinctive range of the heat ($\leqslant 40$ kJ mol$^{-1}$) of physically adsorbed species [28]. This is quite consistent with a weak type of bonding of the pyridine to silica surfaces, namely hydrogen bonds and dispersion forces. This also applies to the $\Delta H$ values calculated for the desorption of PPy and HPy from alumina surfaces ($\leqslant 35.5$ kJ mol$^{-1}$). However, the $\Delta H$ values for the desorption of IPy (238.3 kJ mol$^{-1}$) and LPy (326.9 kJ mol$^{-1}$) are consistent with the stronger type of bonding involved [28].

Specifically, however, it is interesting that relatively lower $\Delta H$ values (15.8 and 28.4 kJ mol$^{-1}$) were obtained for the desorption of the HPy species (II and I) from silica than (35.5 kJ mol$^{-1}$) for the desorption of the same species from alumina. This may account for the relatively stronger B sites on alumina than on silica. However, the $\Delta H$ value (15.3 kJ mol$^{-1}$) calculated for the desorption of the CPy species from silica is lower than that (28.5 kJ mol$^{-1}$) calculated for the desorption of the same species from alumina, although both values are less than the latent heat of vapourization of liquid pyridine (35.4 kJ mol$^{-1}$) [29]. CPy is meant to indicate capillary condensed pyridine in the surface pores [30] and thus it is tempting to suggest that CPy is organized in a rather more liquid-like phase on alumina than on silica; the difference may be attributed to the different pore sizes of the two surfaces [30].

It is worth noting that the baseline of the DSC curve of alumina suffers a considerable endothermic drift at > 200°C (Fig. 2). The drift is shown (Fig. 2) to be largely corrected, dealing with Py/Al. Tentatively, one may consider the correction as due to an exothermic process pertinent to the chemical modification of pyridine on alumina [23].

## CONCLUSIONS

Gravimetry and differential scanning calorimetry of the temperature-programmed desorption of an adsorbed base molecule can provide quantitative information about the concentration and strength of acid sites exposed on the adsorbent surface. This is, however, only true provided that the following requirements are fulfilled: (i) a chemically stable, hard base molecule is used as a probe, so that interaction can occur with both weak and strong acid sites; (ii) the adsorbent is thermally stable and does not suffer any significant bulk or surface changes during the measurements; (iii) the measurements are carried out in a dynamic atmosphere of inert gas in order to avoid atmospheric oxidation of the adsorbate; (iv) the adsorbent is pretreated and exposed to the adsorbate in situ; (v) the measurement is made on the adsorbent before and after exposure to the adsorbate; (vi) the measurements are carried out with sufficiently high sensitivity, because the events to be monitored are due to minute amounts of material (surface species); and (vii) the characteristic thermal events (weight-loss steps and heat-input-rate peaks) are well resolved, or can be resolved technically.

## REFERENCES

1 K. Tanabe, Solid Acids and Bases: Their Catalytic Properties, Academic Press, London, 1970.
2 B. Imelik et al. (Eds.), Catalysis by Acids and Bases, Elsevier, Amsterdam, 1985.
3 B. Delmon et al. (Eds.), Preparation of Catalysts II, Elsevier, Amsterdam, 1979.
4 M. Che and L. Benneviot, Z. Phys. Chem. (NF), 152 (1987) 113.
5 B.S. Goldstein, Experimental Methods in Catalysis Research, Academic Press, London, 1968.
6 F. Forni, Catal. Rev., 8 (1973) 65.
7 E.A. Paukshtis and E.N. Yurchenko, Russ. Chem. Rev. (Engl. Trans.), 52 (1983) 242, and references cited therein.
8 L.H. Little, Infrared Spectra of Adsorbed Species, Academic Press, London, 1966.
9 M.L. Hair, Infrared Spectroscopy in Surface Chemistry, Marcel Dekker, New York, 1967.
10 R.L. Stone and H.F. Rase, Anal. Chem., 29 (1957) 1273.
11 T. Shirasaki, M. Mimura and K. Mukaida, Bunseki Kiki (Jpn.), 5 (1968) 59.
12 H.-P. Boehm and H. Knözinger, in J.R. Anderson and M. Boudart (Eds.), Catalysis—Science and Technology, Vol. 4, Springer-Verlag, Berlin, 1983, pp. 39–207.
13 J.W. Dodd and K.H. Tonge, in B.R. Currell (Ed.), Thermal Methods, Wiley, London, 1987, p. 142.
14 N.E. Fouad, H. Knözinger, M.I. Zaki and S.A.A. Mansour, Z. Phys. Chem. (NF), 171 (1991) 75.
15 H. Knözinger, in P. Schuster et al. (Eds.), The Hydrogen Bond, Vol. III, North-Holland, Amsterdam, 1976, pp. 1263–1364.
16 H. Knözinger and P. Ratnasamy, Catal. Rev. Sci. Eng., 17 (1978) 31.
17 G.J. Young, J. Colloid Sci., 13 (1975) 67.
18 H. Knözinger, in B. Imelik et al. (Eds.), Catalysis by Acids and Bases, Elsevier, Amsterdam, 1985, pp. 111–125.
19 J.B. Peri, J. Phys. Chem., 69 (1965) 211, 220, 231.
20 M.I. Zaki and H. Knözinger, Mater. Chem. Phys., 17 (1987) 201.
21 J. Leyrer, B. Vielhaber, M.I. Zaki, Zhuang Shuxian, J. Weitkamp and H. Knözinger, Mater. Chem. Phys., 13 (1985) 301.
22 T.H. Ballinger and J.T. Yates, Jr., J. Phys. Chem., (1991) in press.
23 H. Knözinger, Adv. Catal., 25 (1976) 184.
24 S. Soled, J. Catal., 18 (1983) 252.
25 S.J. Gregg and K.S.W. Sing, Adsorption, Surface Area and Porosity, 2nd edn, Academic Press, London, 1982, pp. 248–282.
26 T.P. Beebe, P. Gelin and J.T. Yates, Jr., Surf. Sci., 148 (1984) 526.
27 E.P. Parry, J. Catal., 2 (1963) 371.
28 H. Knözinger, Adv. Catal., 25 (1976) 1–38.
29 J.A. Dean (Ed.), Lange's Handbook of Chemistry, 11th edn., McGraw-Hill, New York, 1973, p. 9–(95).
30 H. Knözinger, Adv. Catal., 25 (1976) 112–121.